



Effect of reaction parameters on WO_x nanostructures by the solvothermal process

Efecto de los parámetros de reacción en nanoestructuras de WO_x por el proceso solvotermal

Amelia Olivas Sarabia ¹, Marlene N Cardoza-Contreras ², Marcos Alan Cota-Leal ¹, Selene Sepúlveda Guzmán ³

¹Centro de Nanociencias y Nanotecnología, Universidad Nacional Autónoma de México, Km 107 carretera Tijuana-Ensenada, CP. 22860, Ensenada, Baja California, México

²Posgrado de Ciencia e Ingeniería de Materiales, Centro de Nanociencias y Nanotecnología, Universidad Nacional Autónoma de México, Km 107 carretera Tijuana-Ensenada, CP. 22860, Ensenada, Baja California, México

³Centro de Innovación, Investigación y Desarrollo en Ingeniería y Tecnología, Universidad Autónoma de Nuevo León, Avenida Alianza 101 Sur KM. 10 de la nueva carretera internacional de Monterrey, PIIT Monterrey, CP. 66600, Apodaca, Nuevo León, México

Corresponding author: Amelia Olivas Sarabia, Centro de Nanociencias y Nanotecnología, Universidad Nacional Autónoma de México, Km 107 carretera Tijuana-Ensenada, CP. 22860, Ensenada, Baja California, México. E-mail: aolivas@cnyun.unam.mx. ORCID: 0000-0001-7748-2579.

Recibido: 13 de Mayo del 2021

Aceptado: 13 de Septiembre del 2021

Publicado: 24 de Septiembre del 2021

Abstract. - *In this work, nanowires and nanorods of WO_x have been synthesized by the solvothermal method. The effect of reaction time and acetic acid as solvent were studied. X-ray diffraction (XRD) patterns showed the monoclinic WO_{2.72}, WO_{2.79} and orthorhombic WO₃ crystalline structures. Scanning Electron Microscopy (SEM) and High-Resolution Transmission Electronic Microscopy (HRTEM) images presented nanostructures such as nanowires and nanorods at different sizes. Band gap energies were supplied by Ultra Violet visible (UV-vis) absorption spectra. The Photoluminescence (PL) spectra exhibited three emission peaks in the blue zone at 440, 460 and 484 nm. X-ray Photoelectron Spectroscopy (XPS) were used to calculate W₆₊, W₅₊ and W₄₊ oxidation states. The results showed that increasing the reaction time from 10 h to 24 h affected the crystalline structure from monoclinic to orthorhombic. Moreover, with the addition of acetic acid as solvent, the crystal structure is not affected, but stabilizes the monoclinic phase in the course of time.*

Keywords: Acetic acid; WO_x nanowires; Solvothermal; Optical properties.

Resumen. - *En este trabajo se han sintetizado nanocables y nanovarillas de WO_x por el método solvotermal. Se estudió el efecto del tiempo de reacción y del ácido acético como disolvente. Los patrones de difracción de rayos X (XRD) mostraron las estructuras cristalinas monoclinicas WO_{2.72}, WO_{2.79} y ortorrómbicas WO₃. Las imágenes de microscopía electrónica de barrido (SEM) y microscopía electrónica de transmisión de alta resolución (HRTEM) presentaron nanoestructuras como nanocables y nanobarras de diferentes tamaños. Las energías de banda prohibida fueron suministradas por espectros de absorción ultravioleta visible (UV-vis). Los espectros de fotoluminiscencia (PL) exhibieron tres picos de emisión en la zona azul a 440, 460 y 484 nm. Se utilizó espectroscopía de fotoelectrones de rayos X (XPS) para calcular los estados de oxidación W₆₊, W₅₊ y W₄₊. Los resultados mostraron que el aumento del tiempo de reacción de 10 h a 24 h afectaba la estructura cristalina de monoclinica a ortorrómbica. Además, con la adición de ácido acético como disolvente, la estructura cristalina no se ve afectada, pero estabiliza la fase monoclinica con el paso del tiempo.*

Palabras clave: Ácido acético; Nanocables de WO_x; Solvotermal; Propiedades ópticas.



1. Introduction

Nanostructures of metal oxide semiconductors are highly attractive due to their optical and electronic applications. Tungsten oxides have *n*-type conductivity with an indirect wide band gap which ranges from 2.5 to 2.8 eV [1], and have been of great interest because of promising chemical and physical properties. In the last decades, tungsten oxides have been paid great attention as a consequence of their possible applications in electro-chromic devices [2], gas sensors [3], field emission display [4], catalyst [5], [6] and electronic devices of nanostructures [7]. Many methods have been developed to synthesize 1-D nanostructures, such as chemical vapor deposition [8], pulsed-laser deposition [9], [10], template assisted growth [11], thermal annealing [12] and solvothermal synthesis [13], [14]. The solvothermal synthesis is the most simple and effective method due to low temperature growth of nanostructures and low cost. Here, we report the synthesis and characterization of tungsten oxide nanorods and nanowires by solvothermal method varying reaction parameters.

2. Experimental

Metal alkoxides are derivated from alcohols that can be easily removed by hydrolysis and heating treatment in order to obtain high purity metallic oxides. In usual methods, metal alkoxides are synthesized by direct reaction of reactive metals and alcohols [15]. Ethanol and acetic acid as a solvent have been used in metallic oxides nanostructures principally to favor an esterification reaction between acetic acid and an alcohol that influences the formation of a certain type of metallic oxide modifying the reactivity of the metal alkoxide [16], [17]. In this method, reacts homogeneously with a water molecule

which is condensed from an esterification process as follows:



A starting solution of 25 mM of tungsten hexachloride (99.99%, WCl_6 , Sigma-Aldrich) was added in 38 mL of ethanol (99.8% HPLC, Sigma-Aldrich). The prepared solution was transferred to a 45 mL teflon-lined stainless steel autoclave. Solvothermal synthesis was conducted at 200 °C using an electric oven. Two experiments were carried out varying the reaction time for 10 h and 24 h. After reaction, the autoclave was cool down at room temperature. After the above, a blue precipitate was collected and washed with ethanol, and then dried at 80 °C. In a different approach, 0.5 mL of acetic acid (ACS reagent, $\geq 99.7\%$, Sigma-Aldrich) was added to the precursor solution (WCl_6 /ethanol) and the solvothermal reaction was conducted at 200 °C for 10 h and 24 h. Structural characterization and morphology were studied by X-ray diffraction, XRD (Diffractometer Rigaku, Geigerflex D/Max), scanning electron microscopy, SEM (FEI NOVA 200 NANOSEM) and high-resolution transmission electron microscope, HRTEM (JEOL-2010). Finally, ultra violet visible, UV-vis, absorption spectra for all the as-prepared WO_x samples were carried out using a VARIAN CARY 300 double beam UV-Vis's spectrophotometer. X-ray photoelectron spectroscopy, XPS (SPECS) was used to analyzing oxygen vacancies in the samples.

3. Results and discussion

3.1 Structural analysis

Figure 1 depicts the XRD patterns of the tungsten oxide nanostructures synthesized at different solvothermal reaction conditions. The XRD



suggest that the nanowires grow as single crystals with a preferential growth along the $\langle 010 \rangle$ direction. The HRTEM image for the sample prepared at 24 h of reaction time shows nanowires with 8 nm of average diameter size

and nanorods with diameters ranging from 50 to 150 nm, Figure 2 (b). The respective HRTEM image (Figure 3f) shows nanowires that grow along the $\langle 001 \rangle$ direction.

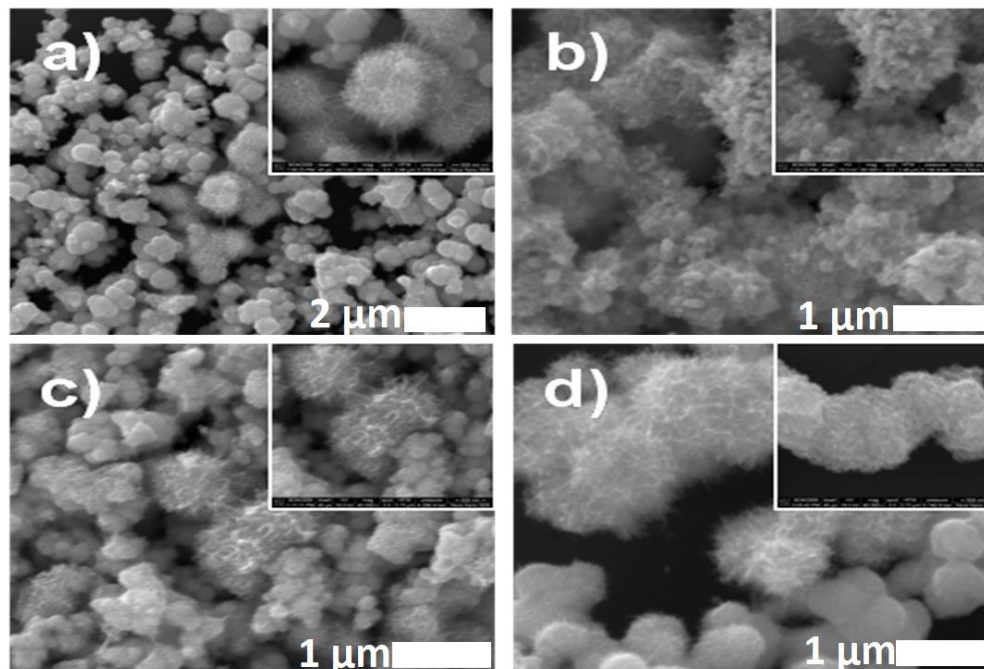


Figure 2. SEM images of synthesized tungsten oxide nanostructures. WCl_6 /ethanol system at (a) 10 h and (b) 24 h respectively. WCl_6 /ethanol/acetic acid system at (c) 10 h and (d) 24 h respectively. Insets show images of high magnification.

The HRTEM image of the sample prepared using acetic acid as additive and at 10 h of reaction time is presented in Figure 3 (c). The presence of nanowires aggregates with diameter size ranging from 200-300 nm was also observed. In addition, the diameter size of the nanowires was 4 nm. When the reaction was carried out at 24 h of reaction time the average diameter size of nanowires in the hiperbranched arrays increased to 7 nm, Figure 3 (d).

Based on SEM, TEM, HRTEM and XRD results we propose a possible WO_x nanowires growth mechanism. For the case of the first conditions or only ethanol as solvent and 10 h of reaction, reaction situation bring about the formation of the $WO_{2.79}$ nucleus given the conventional mechanism of growth and nucleation, rendering

the monoclinic phase. As soon as the temperature get to the 200 °C and the nucleus has reached optimums size to not dissolve, the production of these particles continues. During the growth process, the nanowires display an epitaxial growth in the $\langle 010 \rangle$ direction as single crystals, in agreement to the results obtained by HRTEM, Figure 3(e) [18]. As the reaction continues, the high surface energy of nanowires is passivated by self-assembly and form spherical aggregates. When the reaction is kept for 24 h, the concentration of the number of growing species diminished and at solvothermal conditions the system enters into the Ostwald ripening regime, which favors the formation of nanorods and aggregation arrays like hiperbranched particles. Recent DFT studies have revealed that the creation of vacancies and defects is energetically



unfavorable in monoclinic compounds [19]. This prompted us look for the formation of vacancies for both orthorhombic and monoclinic phases and it is larger for the orthorhombic phase due to the deficiencies of oxygen. This suggests that, the orthorhombic phase to be more stable. The above

can explain the driving force behind the phase formation and the transformation behavior from monoclinic to orthorhombic observed in these materials [20].

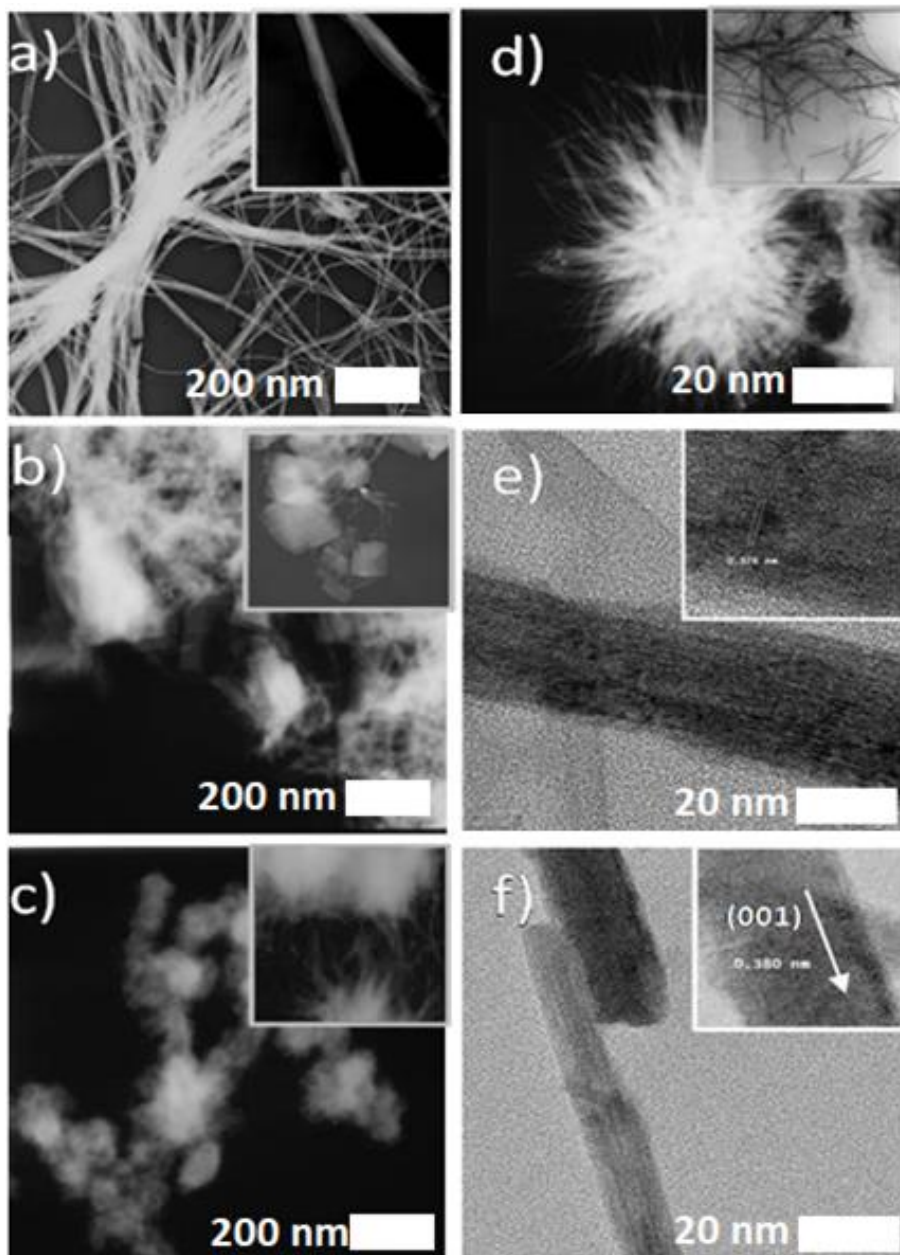


Figure 3. HRTEM images of synthesized tungsten oxide nanostructures. WCl_6 /ethanol system at (a,e)10 h and (b,f) 24 h, respectively. WCl_6 /ethanol/acetic acid system at (c) 10 h and (d) 24 h.



More studies on both phases could be done like Differential Scanning Calorimetry (DSC) curves of thermodynamic field [21] but these are beyond the scope of this work. For the case when acetic acid was added and 10 h of reaction,

3.2 Optical measurements

3.2.1. UV-Vis absorption

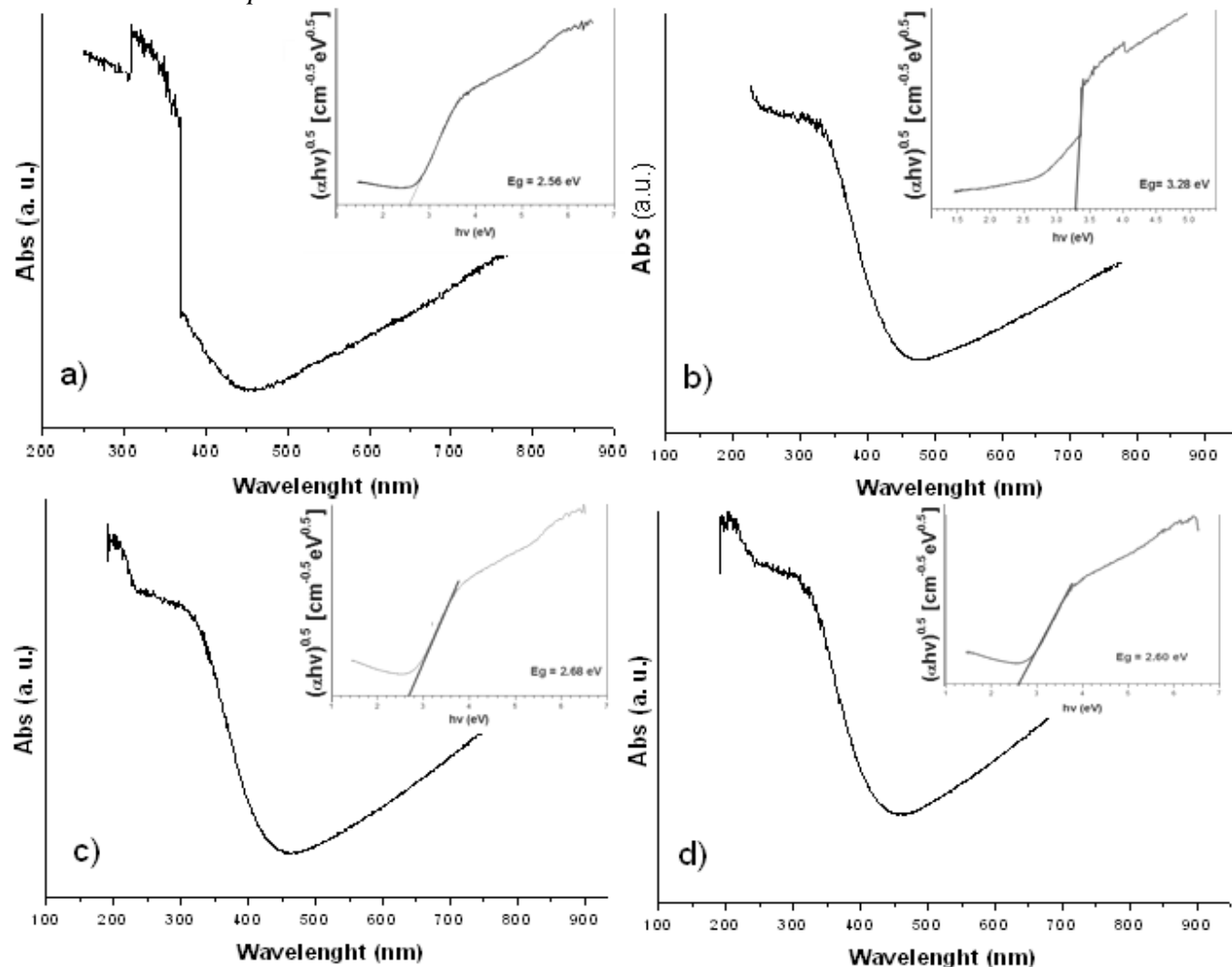


Figure 5. UV-Vis spectra of the obtained WO_x from a) WCl₆/ethanol 10 h b) WCl₆/ethanol/acetic acid 10 h c) WCl₆/ethanol 24 h and d) WCl₆/ethanol/acetic acid 24 h reaction conditions.

Optical band gap can be obtained from the UV region by means of the fundamental absorption edge or coefficient and it is determined by considering an indirect transition between the 2p

Figure 5 shows the UV-vis absorption spectra for all the as-prepared WO_x samples. Here a slide of maximum absorption to UV region can be observed, which suggests a quantum confinement effect due to the presence of nanometer size particles.

electrons from the valence band of the oxygen and the 5d conduction bands of tungsten [22]. The optical band gap is formally described as the intercept of the plot of $(\alpha hv)^{1/2}$ against $h\nu$, where



α and $h\nu$ denote the absorption coefficient and photon energy [23], respectively. The obtained

WO_x nanostructures band gap energies and particle sizes are presented in Table 1.

Table 1. Band gap energies and particle sizes of WO_x nanostructures for both systems

System	E _g (eV)	Particle size (nm)
WCl6/ethanol 10 h	2.56 (484 nm)	10
WCl6/ethanol 24 h	2.68 (463 nm)	8
WCl6/ethanol/acetic acid 10 h	3.28 (378 nm)	4
WCl6/ethanol/acetic acid 24 h	2.60 (477 nm)	7

As can be observed from Table 1, the quantum size effect optical band gap value increases when the average particle size decreased, this is possible due to the quantum confinement size. The higher band gap energy value was the one from the WO_x obtained using acetic acid as an additive at 10 h with an average diameter size of 4 nm.

3.2.2. Photoluminescence (PL) spectra

In order to study the optical properties of the synthesized nanostructures we used the PL spectra. The WO_x prepared under hydrothermal conditions at 10 and 24 h exhibit three emission peaks in the blue zone at 440, 460 and 484 nm. The blue emission observed for WO_x has not been completely clarified, but several works have focused in its study. The emissions at 484 nm and 460 nm are attributed to the indirect band to band transition of tungsten oxide, according to the values of band gap energies for WO_{2.72} nanowires (2.56 eV) and WO₃ nanowires/nanorods (2.68 eV) for the samples prepared under hydrothermal conditions at 10 and 24 hours of reaction time, respectively. On the other hand, the transitions in the blue region have been assumed as a result of the presence of oxygen vacancies in the structure of the WO_{3-x} nanowires. According to studies carried out by Jian Yi, *et al.* [24]. The emissions of three-dimensional nanowires nets are

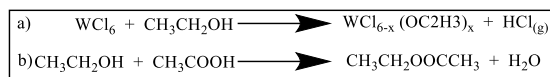
attributed to structural and surface defects based on non-stoichiometric tungsten oxide (WO_{3-x}). Also, the spectra for the products prepared using acetic acid as additive at 10 and 24 h of reaction time are presented in figure 5 (a). The sample prepared at 10 h presents PL emission very similar to the sample prepared without acetic acid with 3 emission shoulders at 439, 458 and 484 nm. Nevertheless, in the sample synthesized at 24 h in presence of acetic acid an intense UV emission at 380.5 nm was observed, besides the emission in the visible region, figure 5 (b). This UV emission is not typical; nevertheless it already has been reported by J. Wang, *et al* [25]. These authors studied the luminescence of WO₃ nanosheets obtaining two emissions in the UV region which were attributed to oxygen vacancies. To obtain major information about the presence of these oxygen vacancies, the samples were analyzed by XPS using monochromatized Al-K α radiation with photon energy of 1486.6 eV.

The XPS spectra for the W_{4f} and O_{1s} peaks for the WO_x prepared under solvothermal conditions at 10 and 24 h are shown in figure 6 (a) and (b), respectively. At 10 h the XPS spectra showed that the peak for O_{1s} was at 530.35 eV. 4f peaks binding energies were at 38.0 and 36.0 eV, which corresponds to spin-orbit splitting of the W 4f_{7/2} and W 4f_{5/2} components, respectively [30]. W⁶⁺,



W^{5+} and W^{4+} oxidation states of the W_{4f} peak depict to the $WO_{2.72}$ phase. These results are consistent to Angelis, B. A. and Karuppanan S. [26], [27]. While at 24 h only the W_{6+} and W_{5+} oxidation states appear in the W_{4f} peak deconvolution which agrees with literature reported for the WO_3 phase [27]. The peak position for O1s at 24 h was 530.4 eV. The XPS collected spectra data for both systems is showed in table 2. The compositional stoichiometry O/W was calculated from the relative intensities of the XPS spectra of all procedures and showed in Table 2.

Here, one can observe that all the samples have oxygen deficiencies. This is definitively due to the presence of oxygen vacancies which are common in WO_x structures. It is necessary to mention that the sample corresponding to the WCl_6 /ethanol/acetic acid system at 24 h is the one that has a high deficiency of oxygen ($O/W=0.7$) and also the one that has the highest concentration of W^{5+} (40.02%). This supports the photoluminescence results where the same sample presents an intense emission in the UV region also presents a higher concentration of oxygen vacancies. A possible explanation to this is that in the WO_x sample prepared using acetic acid as additive during esterification reaction water molecules were generated and they can hydrolyze the $WCl_{6-x}(OC_2H_3)_x$ complexes which were produced in the reaction between WCl_6 and ethanol. Here the W^{6+} can be reduced to W^{5+} during the oxidative esterification reaction of ethanol in ethyl acetate (see Scheme 1). This way one can expect that the addition of acetic acid to the precursor solution WCl_6 /ethanol causes a major concentration of W^{5+} in the final product in function of the time.



Scheme 1. (a) Reaction between tungsten hexachloride and ethanol, (b) esterification reaction between ethanol and acetic acid.

4. Conclusions

WO_x nanowires were obtained by using a simple solvothermal method varying the reaction time and the use of acetic acid as an additive in the precursor solution. XRD patterns showed the monoclinic $WO_{2.79}$ and orthorhombic WO_3 phases. SEM and TEM images showed nanowires (500 nm-1.5 μ m) and nanorods (55-65 nm) structures. UV-Vis absorption presented a range of band gap energies depending of the particle size (4 nm-3.28 eV) and (10 nm-2.56 eV). The PL spectra exhibited three emission peaks in the blue zone at 440, 460 and 484 nm. W^{6+} , W^{5+} and W^{4+} oxidation states of the W_{4f} peak depict to the $WO_{2.72}$ phase were supplied by XPS. The results showed that increasing the reaction time from 10 h to 24 h affected the crystalline structure changing from monoclinic to orthorhombic. Moreover, with the addition of acetic acid as solvent, the crystal structure is not affected, but stabilizes the monoclinic phase in the course of time.

5. Authorship acknowledgement

Amelia Olivas Sarabia: Resources; Supervision; Project administration; Funding acquisition. *Marlene N Cardoza-Contreras:* Methodology; Investigation. *Gonzalo Lastra Medina:* Writing - Original Draft. *Marcos Alan Cota-Leal:* Writing - Review & Editing. *Selene Sepúlveda Guzmán:* Methodology; Resources; Supervision.

6. Acknowledgements

The authors are grateful to F. Ruiz, Israel Gradilla, E. Aparicio and E. Flores from CNYN-



UNAM and to F. Brown from UNISON for their technical assistance, and PAPIT-UNAM project number IN107220 for their financial aid. M. A. Cota-Leal gratefully acknowledges the postdoctoral grant from the DGAPA-UNAM program.

References

[1] M. Ling, C. S. Blackman, R. G. Palgrave, C. Sotelo-Vazquez, A. Kafizas, and I. P. Parkin, "Correlation of Optical Properties, Electronic Structure, and Photocatalytic Activity in Nanostructured Tungsten Oxide," *Adv. Mater. Interfaces*, vol. 4, no. 18, p. 1700064, Sep. 2017. <https://doi.org/10.1002/admi.201700064>

[2] D. Ma, T. Li, Z. Xu, L. Wang, and J. Wang, "Electrochromic devices based on tungsten oxide films with honeycomb-like nanostructures and nanoribbons array," *Sol. Energy Mater. Sol. Cells*, vol. 177, no. December 2016, pp. 51-56, Apr. 2018. <https://doi.org/10.1016/j.solmat.2017.06.009>

[3] C. Dong, R. Zhao, L. Yao, Y. Ran, X. Zhang, and Y. Wang, "A review on WO₃ based gas sensors: Morphology control and enhanced sensing properties," *J. Alloys Compd.*, vol. 820, p. 153194, Apr. 2020. <https://doi.org/10.1016/j.jallcom.2019.153194>

[4] J. Liu, Z. Zhang, Y. Zhao, X. Su, S. Liu, and E. Wang, "Tuning the Field-Emission Properties of Tungsten Oxide Nanorods," *Small*, vol. 1, no. 3, pp. 310-313, Mar. 2005. <https://doi.org/10.1002/sml.200400054>

[5] H. Quan, Y. Gao, and W. Wang, "Tungsten oxide-based visible light-driven photocatalysts: crystal and electronic structures and strategies for photocatalytic efficiency enhancement," *Inorg.*

Chem. Front., vol. 7, no. 4, pp. 817-838, 2020. <https://doi.org/10.1039/C9QI01516G>

[6] W.-L. Dai, J. Ding, Q. Zhu, R. Gao, and X. Yang, "Tungsten containing materials as heterogeneous catalysts for green catalytic oxidation process," in *Catalysis*, vol. 28, 2016, pp. 1-27. <https://doi.org/10.1039/9781782626855-00001>

[7] Z. Hai, Z. Wei, C. Xue, H. Xu, and F. Verpoort, "Nanostructured tungsten oxide thin film devices: from optoelectronics and ionics to iontronics," *J. Mater. Chem. C*, vol. 7, no. 42, pp. 12968-12990, 2019. <https://doi.org/10.1039/C9TC04489B>

[8] N. C. Ou, X. Su, D. C. Bock, and L. McElwee-White, "Precursors for chemical vapor deposition of tungsten oxide and molybdenum oxide," *Coord. Chem. Rev.*, vol. 421, p. 213459, Oct. 2020. <https://doi.org/10.1016/j.ccr.2020.213459>

[9] P. Huang, M. M. Ali Kalyar, R. F. Webster, D. Cherns, and M. N. R. Ashfold, "Tungsten oxide nanorod growth by pulsed laser deposition: influence of substrate and process conditions," *Nanoscale*, vol. 6, no. 22, pp. 13586-13597, 2014. <https://doi.org/10.1039/C4NR03977G>

[10] M. Fendrich, Y. Papat, M. Orlandi, A. Quaranta, and A. Miotello, "Pulsed laser deposition of nanostructured tungsten oxide films: A catalyst for water remediation with concentrated sunlight," *Mater. Sci. Semicond. Process.*, vol. 119, no. May, p. 105237, Nov. 2020. <https://doi.org/10.1016/j.mssp.2020.105237>

[11] M. Sadakane, K. Sasaki, H. Kunioku, B. Ohtani, W. Ueda, and R. Abe, "Preparation of nano-structured crystalline tungsten(vi) oxide and enhanced photocatalytic activity for



decomposition of organic compounds under visible light irradiation," *Chem. Commun.*, vol. 1, no. 48, p. 6552, 2008. <https://doi.org/10.1039/b815214d>

[12] S. Jeon and K. Yong, "Direct synthesis of W18O49 nanorods from W2N film by thermal annealing," *Nanotechnology*, vol. 18, no. 24, p. 245602, Jun. 2007. <https://doi.org/10.1088/0957-4484/18/24/245602>

[13] H. G. Choi, Y. H. Jung, and D. K. Kim, "Solvothermal Synthesis of Tungsten Oxide Nanorod/Nanowire/Nanosheet," *J. Am. Ceram. Soc.*, vol. 88, no. 6, pp. 1684-1686, Jun. 2005. <https://doi.org/10.1111/j.1551-2916.2005.00341.x>

[14] M. Juelsholt, T. Lindahl Christiansen, and K. M. Ø. Jensen, "Mechanisms for Tungsten Oxide Nanoparticle Formation in Solvothermal Synthesis: From Polyoxometalates to Crystalline Materials," *J. Phys. Chem. C*, vol. 123, no. 8, pp. 5110-5119, Feb. 2019. <https://doi.org/10.1021/acs.jpcc.8b12395>

[15] L. Klein, *Handbook of Sol-Gel Science and Technology*. Cham: Springer International Publishing, 2017. <https://doi.org/10.1007/978-3-319-19454-7>

[16] C. Wang, Z.-X. Deng, and Y. Li, "The Synthesis of Nanocrystalline Anatase and Rutile Titania in Mixed Organic Media," *Inorg. Chem.*, vol. 40, no. 20, pp. 5210-5214, Sep. 2001. <https://doi.org/10.1021/ic0101679>

[17] M. Gotić and S. Musić, "Synthesis of Nanocrystalline Iron Oxide Particles in the Iron (III) Acetate/Alcohol/Acetic Acid System," *Eur. J. Inorg. Chem.*, vol. 2008, no. 6, pp. 966-973, Feb. 2008. <https://doi.org/10.1002/ejic.200700986>

[18] J. A. Hollingsworth, "Semiconductor Nanocrystal Quantum Dots," in *Encyclopedia of Inorganic and Bioinorganic Chemistry*, Chichester, UK: John Wiley & Sons, Ltd, 2011. <https://doi.org/10.1002/9781119951438.eibc0261>

[19] J. M. Clark et al., "High voltage sulphate cathodes $\text{Li}_2\text{M}(\text{SO}_4)_2$ (M = Fe, Mn, Co): atomic-scale studies of lithium diffusion, surfaces and voltage trends," *J. Mater. Chem. A*, vol. 2, no. 20, pp. 7446-7453, 2014. <https://doi.org/10.1039/C3TA15064J>

[20] H. Wang, Y. Shi, Z. Li, W. Zhang, and S. Yao, "Synthesis and electrochemical performance of Co_3O_4 /graphene," *Chem. Res. Chinese Univ.*, vol. 30, no. 4, pp. 650-655, Aug. 2014. <https://doi.org/10.1007/s40242-014-4109-8>

[21] A. V. Radha, L. Lander, G. Rousse, J. M. Tarascon, and A. Navrotsky, "Thermodynamic stability and correlation with synthesis conditions, structure and phase transformations in orthorhombic and monoclinic $\text{Li}_2\text{M}(\text{SO}_4)_2$ (M = Mn, Fe, Co, Ni) polymorphs," *J. Mater. Chem. A*, vol. 3, no. 6, pp. 2601-2608, 2015. <https://doi.org/10.1039/C4TA05066E>

[22] C. Granqvist et al., "Recent advances in electrochromics for smart windows applications," *Sol. Energy*, vol. 63, no. 4, pp. 199-216, Oct. 1998. [https://doi.org/10.1016/S0038-092X\(98\)00074-7](https://doi.org/10.1016/S0038-092X(98)00074-7)

[23] S. K. Deb, "Optical and photoelectric properties and colour centres in thin films of tungsten oxide," *Philos. Mag.*, vol. 27, no. 4, pp. 801-822, Apr. 1973. <https://doi.org/10.1080/14786437308227562>



[24] J. Y. Luo et al., "Ultraviolet-visible emission from three-dimensional WO_3-x nanowire networks," Appl. Phys. Lett., vol. 91, no. 9, p. 093124, Aug. 2007.
<https://doi.org/10.1063/1.2776862>

[25] J. Wang, P. S. Lee, and J. Ma, "Synthesis, growth mechanism and room-temperature blue luminescence emission of uniform WO_3 nanosheets with W as starting material," J. Cryst. Growth, vol. 311, no. 2, pp. 316-319, Jan. 2009.
<https://doi.org/10.1016/j.jcrysgr.2008.11.016>

[26] K. Senthil and K. Yong, "Growth and characterization of stoichiometric tungsten oxide nanorods by thermal evaporation and subsequent annealing," Nanotechnology, vol. 18, no. 39, p. 395604, Oct. 2007.
<https://doi.org/10.1088/0957-4484/18/39/395604>

[27] B. A. De Angelis and M. Schiavello, "X-ray photoelectron spectroscopy study of nonstoichiometric tungsten oxides," J. Solid State Chem., vol. 21, no. 1, pp. 67-72, May 1977.
[https://doi.org/10.1016/0022-4596\(77\)90145-1](https://doi.org/10.1016/0022-4596(77)90145-1)



Este texto está protegido por una licencia [Creative Commons 4.0](https://creativecommons.org/licenses/by/4.0/)

Usted es libre para Compartir —copiar y redistribuir el material en cualquier medio o formato— y Adaptar el documento —remezclar, transformar y crear a partir del material— para cualquier propósito, incluso para fines comerciales, siempre que cumpla la condición de:

Atribución: Usted debe dar crédito a la obra original de manera adecuada, proporcionar un enlace a la licencia, e indicar si se han realizado cambios. Puede hacerlo en cualquier forma razonable, pero no de forma tal que sugiera que tiene el apoyo del licenciante o lo recibe por el uso que hace de la obra.

[Resumen de licencia - Texto completo de la licencia](#)